J Biomol NMR (2014) 58:227–230
DOI 10.1007/s10858-014-9819-1

NMR STRUCTURE NOTE

The N-terminal domain of TIR domain-containing adaptor molecule-1, TICAM-1

Hiroyuki Kumeta · Hiromi Sakakibara · Yoshiaki Enokizono · Kenji Ogura · Masataka Horiuchi · Misako Matsumoto · Tsukasa Seya · Fuyuhiko Inagaki

Received: 12 January 2014 / Accepted: 31 January 2014 / Published online: 6 February 2014

Biological context

Toll-like receptors (TLRs) are a family of single-span transmembrane proteins that evoke innate immunity in response to microbial stimuli such as bacterial lipids and non-self nucleic acids (reviewed in Botos et al. 2011 and Kang and Lee 2011). After ligand binding, TLRs oligomerize and undergo conformational changes that induce oligomerization of the cytosolic Toll/interleukin-1 receptor (TIR) domains. This presents a scaffold for the recruitment of downstream TIR domain-containing adaptor molecules.

There are five TIR domain-containing adaptor molecules; myeloid differentiation primary response gene 88 (MyD88), TIR domain-containing adaptor protein (TIRAP) [also known as MyD88 adaptor like (Mal)], TIR domain-containing adaptor molecule-1 (TICAM-1) [also known as TIR domain-containing adaptor-inducing IFN-β (TRIF)], TIR domain-containing adaptor molecule-2 (TICAM-2) [also known as TRIF-related adaptor molecule (TRAM)], and sterile α and huntingtin-elongation-A subunit-TOR armadillo motifs (SARM). Downstream signaling from TLRs is mediated by the association of the TIR domains between receptor and adaptor, and adaptor and adaptor molecules.

TICAM-1 is a signaling adaptor for TLR3 and TLR4 that eventually activates the transcription factors, interferon regulatory factor-3 (IRF-3), NF-κB and AP-1, leading to the induction of type I interferons and inflammatory cytokines (Seya et al. 2005). TLR3 recognizes double-stranded RNA and directly interacts with the TICAM-1 TIR domain via the cytosolic TLR3 TIR domain. TLR4 recognizes lipopolysaccharides together with a cofactor molecule MD2, and interacts with Mal and the TICAM-2 TIR domain via the cytosolic TLR4 TIR domain. Mal and TICAM-2 act as membrane sorting adaptors that interact with MyD88 and TICAM-1, respectively, via TIR domains. In response to TLR stimulation, TICAM-1 alters its distribution profile in the cytosol from diffuse to a speckle-like structure that is indispensable to downstream signaling (Matsumoto et al. 2003; Funami et al. 2007). TICAM-1 consists of an N-terminal domain (NTD), a flexible region that harbors a binding site for tumor necrosis factor receptor-associated factor (TRAF) proteins, a TIR domain, and a C-terminal region that includes the receptor interacting protein 1 (RIP1) binding motif (RHIM). The TIR-domain of TICAM-1 is associated with the TIR domains of TLR3 and TICAM-2, a TLR4-bridging adaptor molecule. The TICAM-1 TIR domain is also involved in TICAM-1 homo-oligomerization (Funami et al. 2008). A TICAM-1 TIR domain mutant (Pro434 substituted to His), defective in homo-oligomerization and diffusively localized in the cytosol, abrogates NF-κB and IRF-3 activation, but retains heterotypic TIR–TIR interaction with TLR3 and TICAM-2 TIRs. Recently, we have determined the structures of the TICAM-1 and TICAM-2 TIR domain mutants (Enokizono et al. 2013). In

H. Kumeta · Y. Enokizono · K. Ogura · F. Inagaki (✉)
Department of Structural Biology, Faculty of Advanced Life Science, Hokkaido University, N-21, W-11, Kita-ku, Sapporo 001-0021, Japan
e-mail: finagaki@pharm.hokudai.ac.jp

H. Sakakibara · M. Horiuchi
Department of Structural Biology, Graduate School of Pharmaceutical Sciences, Hokkaido University, N-12, W-6, Kita-ku, Sapporo 060-0812, Japan

M. Matsumoto · T. Seya
Department of Microbiology and Immunology, Graduate School of Medicine, Hokkaido University, N-15, W-7, Kita-ku, Sapporo 060-8638, Japan

combination with the structural data and yeast two-hybrid experiments using the wild types and several mutants of TICAM-1 and TICAM-2 TIR domain, the interaction site between TICAM-1 and TICAM-2 TIRs was identified.

The TICAM-1 mutant lacking NTD was reported to form a speckle-like signalsome in the cytosol without stimulation and to show interferon-β promoter activity higher than that of the wild-type TICAM-1 (Tatematsu et al. 2010), indicating that NTD interacts with TICAM-1 TIR in an autoinhibitory manner. Here, we report the NMR structure of TICAM-1 NTD and propose an interaction mode between TICAM-1 TIR and NTD.

Methods and results

Sample preparation

TICAM-1 NTD (residue range 1–156) was cloned into the pGEX-6p (GE Healthcare) plasmid. A $^{13}C/^{15}N$ labeled protein was prepared by culturing *E. coli* BL21 cells in stable isotope-labeled C.H.L. medium (Chlorella Industry). Protein expression was induced by the addition of isopropyl-1-thio-β-galactopyranoside to a final concentration of 0.01 mM. After induction, the cells were cultured at 25 °C overnight and then lysed by sonication. The GST-fused protein was purified using a glutathione-Sepharose 4B column (GE Healthcare), and GST was excised from the protein with PreScission protease (GE Healthcare). The protein was further purified by size exclusion chromatography using a Superdex 75 gel filtration column (GE Healthcare). Finally, the protein was concentrated using a Vivaspin 2–5 K ultra filtration system (GE Healthcare).

NMR assignment and structure calculation

NMR experiments were carried out at 25 °C on Varian UNITY INOVA 800 and 600 spectrometers. Measurements for structural analysis were made using a 0.75 mM protein sample resolved in 50 mM Na-phosphate buffer (pH 6.5), containing 3 mM DTT and 1 mM sodium azide. Three dimensional amide-proton-detected spectra; HN(CO)CA, HNCA, CBCA(CO)NH, HNCACB, HBHA(CO)NH, HN(CA)HA, and C(CO)NH, were obtained with a non-uniform sampling schedule method and processed using the rnmrtk program (Mobli et al. 2007). [$^{1}H–^{15}N$] HSQC, [$^{1}H–^{13}C$] HSQC, HC(C)H–TOCSY, ^{13}C-edited NOESY–HSQC and ^{15}N-edited NOESY–HSQC spectra, obtained using a normal sampling schedule, were processed using the NMRpipe program (Delaglio et al. 1995). All spectral analyses were performed with the help of the Sparky program (Goddard and Kneller 1997). The ^{1}H, ^{13}C, and ^{15}N chemical shifts were referenced to DSS in accordance with IUPAC recommendations. The [$^{1}H–^{15}N$] HSQC spectrum of TICAM-1 NTD was well dispersed (Fig. 1), and all the observed $^{1}H/^{15}N$ and $^{1}H/^{13}C$ resonances were assigned except for the side chain $^{1}H/^{15}N$ resonances of Lys and Arg residues. TICAM-1 NTD contains four Cys residues (C^{3}, C^{37}, C^{109}, and C^{144}). The chemical shifts of the β-carbons of these Cys residues indicate that all of these Cys residues exist in reduced state.

Interproton distance restraints for structural calculations were obtained from ^{13}C-edited NOESY–HSQC and ^{15}N-edited NOESY–HSQC spectra using a mixing time of 75 ms. The restraints for backbone ϕ and ψ torsion angles were derived from the chemical shifts of backbone atoms using the TALOS+ program (Shen et al. 2009). The structure determination and NOE assignment were carried out using the

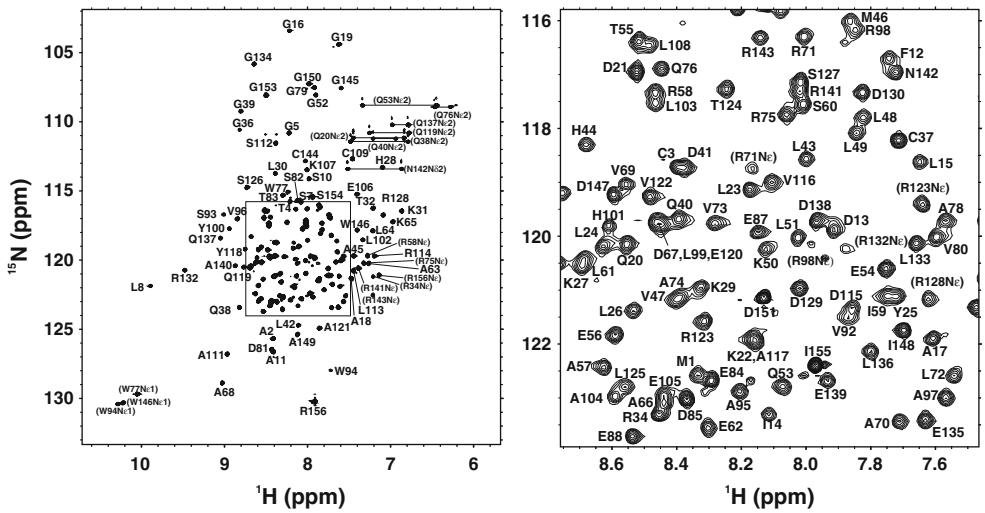

Fig. 1 [$^{1}H–^{15}N$] HSQC spectrum of the TICAM-1 NTD with resonance assignments. The *boxed region* (in *left*) is expanded on the *right*

Table 1 Structural statistics for the TICAM-1 NTD

NOE distance constraints	
Total	3,828
Short range ($\|i - j\| \leq 1$)	1,952
Medium range ($1 < \|i - j\| < 5$)	976
Long range ($\|i - j\| \geq 5$)	900
Number of violations	
Distance > 0.3 Å	3
Angle > 5°	0
Structural coordinates rmsd (Å) (residue range 5–81, 88–150)	
Backbone atoms	0.33
All heavy atoms	0.70
Ramachandran plots (%)	
Most favored regions	78.4
Additionally allowed regions	21.0
Generously allowed regions	0.6
Disallowed region	0.0

CYANA 2.1 software package (Güntert 2004). As an input for the final structural calculation of TICAM-1 NTD, a total of 3,823 distance and 231 dihedral angle restraints were used (Table 1). At each stage, 100 structures were calculated using 30,000 steps of simulated annealing, and a final ensemble of 20 structures was selected based on CYANA target function values. The determined structures were validated by CYANA macros including distance and angle violation and Ramachandran plots. The atomic coordinates and NMR data have been deposited in the Protein Data Bank (PDB code: 2M63) and BMRB (BMRB ID: 19106).

Discussion and conclusions

The solution structure of TICAM-1 NTD

The three-dimensional structure of TICAM-1 NTD was determined using standard hetero-nuclear multidimensional

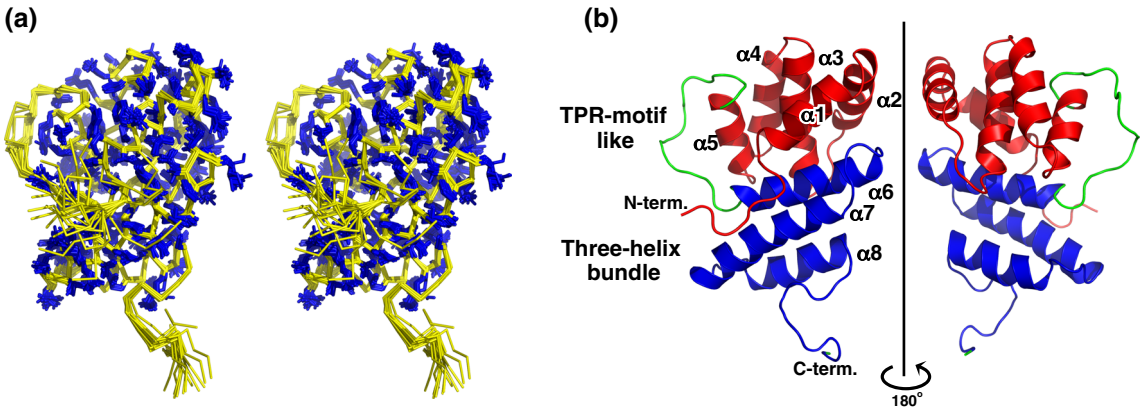

Fig. 2 Solution structure of TICAM-1 NTD. **a** Overlay of the ensemble of 20 final energy-minimized CYANA structures in stereo. Main chain and converged side chains were colored in *yellow* and *blue*, respectively. **b** Ribbon diagrams of the lowest energy structure. TPR-motif like domain, long-loop region and three-helix bundle domain were colored in *red*, *green* and *blue*. Structures were drawn using PyMOL (http://www.pymol.org/)

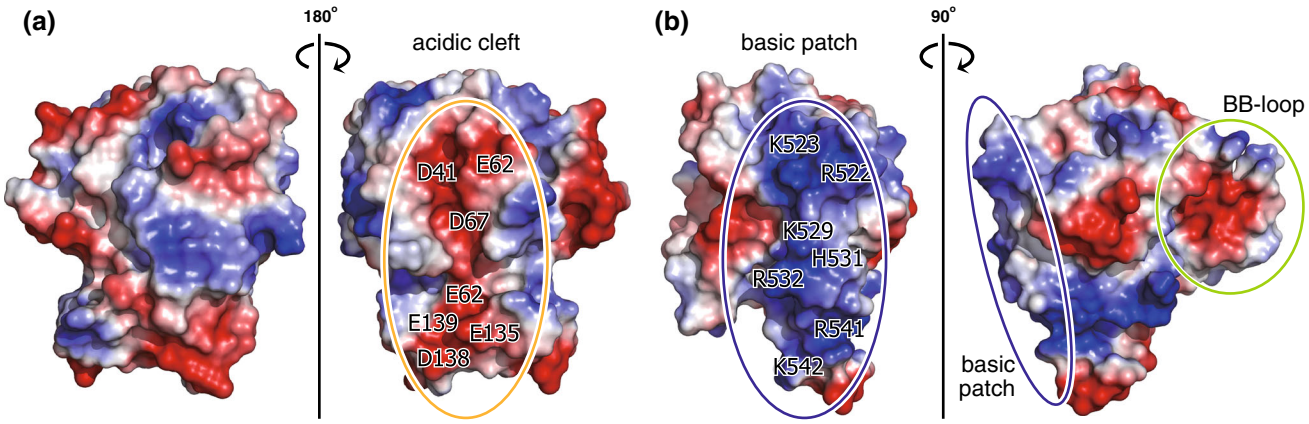

Fig. 3 Electrostatic surface potential mapped on the molecular surface of **a** TICAM-1 NTD (PDB ID: 2M63) and **b** TICAM-1 TIR (PDB ID: 2M1X). Positive and negative charge densities are colored *blue* and *red*, respectively. Surface mapping was drawn using PyMOL with APBS tools

NMR methods. TICAM-1 NTD formed a single, compact domain comprised of eight α-helices (α1: 9–18, α2: 20–31, α3: 38–51, α4: 54–64, α5: 68–76, α6: 92–106, α7: 111–128, and α8: 133–144) and a long loop region between α5 and α6 helices (Fig. 2). In this loop, the region between Ser82 and Glu87 is located that shows low convergence of backbone structure because these residues have no long range NOEs. The overall arrangement of the α-helices in TICAM-1 NTD was found to be novel after an homology search of the previously determined structures using the DALI server (Holm et al. 2008). TICAM-1 NTD can be divided into two segments, a TPR (tetratricopeptide repeat) motif-like region (α1–α5) and a three-helix bundle region (α6–α8). The TPR motif-like region has two sequentially adjacent anti-parallel α-helical pairs (α2–α3 and α4–α5), as is observed in typical TPR proteins. The TPR proteins mediate the protein–protein interactions or inter-domain assembly of multiple domain proteins. The TPR proteins generally present tandem arrays of 3–16 motifs, which form a right-handed super-helical structure and create an amphipathic groove for target recognition. However, the TPR-motif of TICAM-1 NTD does not have sufficient repeats to create a super-helical structure, and moreover, the α1-helix lies on the amphipathic groove (Fig. 2b).

TICAM-1 TIR domain binding site

Recent studies have shown that TICAM-1 NTD is an autorepression domain that directly interacts with the TICAM-1 TIR domain, leading to attenuation of the TIR–TIR interaction (Tatematsu et al. 2010). In a previous paper (Enokizono et al. 2013), we presented the TICAM-1 TIR domain structure and identified two distinct interaction sites required for homotypic and heterotypic TIR oligomerization. A hydrophobic patch that includes the BB loop was important in mediating the homotypic interaction of TICAM-1 TIR, whereas a basic patch on the αE- and αE′-helices was essential for heterotypic interaction with TICAM-2 TIR (Fig. 3b left). An acidic cleft stretched over the TPR motif-like region and three-helix bundle region (Fig. 3a right) that could interact with the basic patch of TICAM-1 TIR domain (Fig. 3b left) was found on the TICAM-1 NTD surface. This suggests the possibility that TICAM-1 NTD blocks the binding between TICAM-1 TIR and TICAM-2 TIR, thus regulating TICAM-1-mediated TLR4 signaling in an autoinhibitory manner. Further studies are required to confirm this hypothesis.

References

Botos I, Segal DM, Davies DR (2011) The structural biology of Toll-like receptors. Structure 19:447–459

Delaglio F, Grzesiek S, Vuister GW, Zhu G, Pfeifer J, Bax A (1995) NMRPipe: a multidimensional spectral processing system based on UNIX pipes. J Biomol NMR 6:277–293

Enokizono Y, Kumeta H, Funami K, Horiuchi M, Sarmiento J, Yamashita K, Standley DM, Matsumoto M, Seya T, Inagaki F (2013) Structures and interface mapping of the TIR domain-containing adaptor molecules involved in interferon signaling. Proc Natl Acad Sci USA 110:19908–19913

Funami K, Sasai M, Ohba Y, Oshiumi H, Seya T, Matsumoto M (2007) Spatiotemporal mobilization of Toll/IL-1 receptor domain-containing adaptor molecule-1 in response to dsRNA. J Immunol 179:6867–6872

Funami K, Sasai M, Oshiumi H, Seya T, Matsumoto M (2008) Homo-oligomerization is essential for Toll/interleukin-1 receptor domain-containing adaptor molecule-1-mediated NF-κB and interferon regulatory factor-3 activation. J Biol Chem 283:18283–18291

Goddard TD, Kneller DG (1997) SPARKY 3, University of California, San Francisco. http://www.cgl.ucsf.edu/home/sparky

Güntert P (2004) Automated NMR structure calculation with CYANA. Methods Mol Biol 278:353–378

Holm L, Kääriäinen S, Rosenström P, Schenkel A (2008) Searching protein structure databases with Dali Lite v. 3. Bioinformatics 24:2780–2781

Kang JY, Lee JO (2011) Structural biology of the Toll-like receptor family. Ann Rev Biochem 80:917–941

Matsumoto M, Funami K, Tanabe M, Oshiumi H, Shingai M, Seto Y, Yamamoto A, Seya T (2003) Subcellular localization of Toll-like receptor 3 in human dendritic cells. J Immunol 171:3154–3162

Mobli M, Maciejewski MW, Gryk MR, Hoch J (2007) Automatic maximum entropy spectral reconstruction in NMR. J Biomol NMR 39:133–139

Seya T, Oshiumi H, Sasai M, Akazawa T, Matsumoto M (2005) TICAM-1 and TICAM-2: toll-like receptor adapters that participate in induction of type 1 interferons. Int J Biochem Cell Biol 37:524–529

Shen Y, Delaglio F, Cornilescu G, Bax A (2009) TALOS+: a hybrid method for predicting protein backbone torsion angles from NMR chemical shifts. J Biomol NMR 44:213–223

Tatematsu M, Ishii A, Oshiumi H, Horiuchi M, Inagaki F, Seya T, Matsumoto M (2010) A molecular mechanism for Toll-IL-1 receptor domain-containing adaptor molecule-1-mediated IRF-3 activation. J Biol Chem 285:20128–20136